J. Jpn. Soc. Powder Powder Metallurgy, **72** (2025) S1283-S1289
https://doi.org/10.2497/jjspm.16D-T18-03

Niobium Carbide-Reinforced Ferrous Matrix Composites: An in situ Powder Metallurgy Approach

Isadora Schramm DESCHAMPS[1*], Daniel dos Santos AVILA [2], Enzo Vanzuita PIAZERA[1], and Aloisio Nelmo KLEIN[1]

[1] Universidade Federal de Santa Catarina (UFSC), Campus Universitário Reitor João David Ferreira Lima, s/n°, Trindade, Florianópolis 88040-900, Brazil

[2] TU Delft, Department of Materials Science and Engineering, Delft University of Technology, Mekelweg 2, 2628 CD Delft, The Netherlands

Abstract

This study focuses on developing a new processing route for ferrous matrix composites reinforced with niobium carbide by producing the reinforcement particles in situ using powder metallurgy. The aim is to improve the interfacial adhesion between matrix and reinforcement compared to traditional ex situ methods. Computational thermodynamics and kinetic analysis were used to optimize the raw materials and processing parameters. The raw materials are mixed, uniaxially pressed, and sintered in a tubular furnace. The study finds that liquid phase sintering improves densification but also leads to clustering, niobium-free regions, and abnormal grain growth. The optimal combination of porosity and microhardness is 16.5 ± 0.7% and 952 ± 82 HV0.05, respectively. Although there is room for further adjustments in processing, this study lays the groundwork for creating valuable materials using Brazilian strategic raw materials and technology.

Keywords: Powder Metallurgy, In situ Composites, Niobium carbide, NbC, Ferrous matrix composite

Introduction

Niobium carbide (NbC) has exceptional thermomechanical properties, including a high melting point (3618°C), high hardness (2200 - 2400 HV0.05), and a modulus of elasticity ranging from 343 to 580 GPa. Traditionally, NbC cermets are made using ex situ methods, where reinforcement particles are mixed with the metal matrix [1–4]. However, these methods often result in issues like poor dispersion, interfacial defects, and low matrix continuity due to the low solubility of NbC in iron. In situ processing techniques have emerged as a solution to these challenges. In situ formation involves synthesizing reinforcements through exothermic reactions during composite fabrication, resulting in clean interfaces and strong adhesion between the matrix and reinforcements [5–7]. This approach is similar to the diffusion alloying technique used in high-performance steels, where Nb-rich iron alloys are atomized and blended with graphite for NbC formation during reactive sintering [8,9].

In this work, we aimed to achieve higher NbC levels compared to diffusion-alloyed steels and smaller carbide sizes compared to existing in situ cermets. Using powder metallurgy, we fabricated a ferrous matrix composite with in situ-generated niobium carbide from Fe_2Nb intermetallic with graphite.

Materials and Methods

The Fe_2Nb powder used in the experiments was synthesized in our laboratory because we have not found commercially available Fe_2Nb powder. The powder was prepared by solid state diffusion using a mixture of FeNb and carbonyl iron powder, aiming at a 55-45 Fe:Nb proportion, which corresponds to Fe_2Nb. 72,35 wt.% milled ferroniobium powder (CBMM, d_{50} = 3μm) and 27.65 wt.% carbonyl iron powder (Sintez, d_{50} = 4,5 μm) were mixed, uniaxially compacted at 700 MPa and heated to 1300 ºC for 1h. The compacts were then re-milld into powder, which has a d_{50} = 3.5 μm, and its composition, determined by energy dispersive X-ray spectroscopy (EDS), is shown in Table 1. X-ray diffraction peaks confirmed that the detected phase corresponds to the diffraction pattern of ICSD 197487 Fe_2Nb Laves.

Table 1: Composition of Fe_2Nb powder

Fe (wt.%)	Nb (wt.%)	Si (wt.%)	Al (wt.%)	Ti (wt.%)
54.2 ± 1.0	44.5 ± 1.0	0.6 ±0.1	0.4 ± 0,1	0.2 ± 0.1

The Fe_2Nb powder was blended with graphite (Micrograf 99501 UJ, d50 = 0.83 μm, 99.95% purity, National do Grafite) in proportions of 5.5, 6.0, 6.5, and 7.0 wt.% and homogenized in a Y-type mixer with steel balls at a 1:1 weight ratio for 45 minutes at 30 rpm. The powder was then granulated in 50 g batches using 2 g of paraffin wax dissolved in 20 mL of hexane and sieved to a size range between 80 and 500 μm. The granulated mixture was uniaxially pressed at 400 MPa in a cylindrical die with a diameter of 9.9 mm. The resulting cylinders were sintered in

*corresponding author, E-mail:isadora.deschamps@labmat.ufsc.br

a hybrid plasma reactor developed by us (WO-2009149526-A1) using the thermal cycle described in Fig. 1.

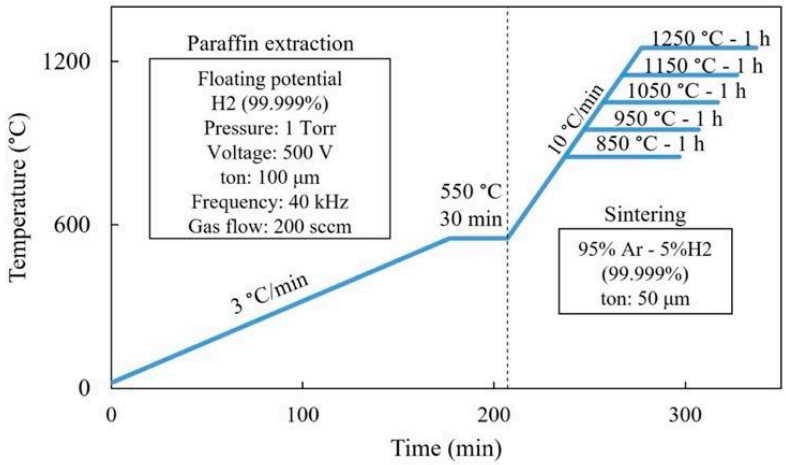

Fig. 1: Sintering parameters used in the plasma reactor.

Phase analysis was performed with a Rigaku Miniflex 600 diffractometer using Cu Kα radiation and refined using the Rietveld method in Maud software. The microstructures and chemical compositions were examined with a TESCAN VEGA3 scanning electron microscope coupled with an Oxford Energy-dispersive X-ray spectrometer. Geometric density of the compacts was measured with a Mettler Toledo XS205 Dual Range precision scale and a Mitutoyo IP65 micrometer. All measurements are averages of at least three samples. Vickers hardness was measured using 1 kg load in a M4C 250 G3 (Emco-Test). The results are the average of two samples with at least three measurements per sample. Vickers microhardness was measured using FUM 800 FM 800 equipment under 50 gf load. The results are the average of two samples with at least five measurements per sample.

Results and Discussion

We simulated using Themo-Calc software and TCFE7 database a Fe_2Nb-C pseudobinary phase diagram (Fig. 2) using the raw material composition of 54.2Fe-44.5Nb-0.6Si-0.4Al-0.2Ti wt.%. By adding sufficient graphite to react with all the available niobium (approximately 5.5 wt.% graphite or ~50 wt.% NbC), the Fe_2Nb-C binary phase diagram resembles an Fe-C binary phase diagram, except that NbC is present in all phase fields. Although the equilibrium phase fields above 5.5 wt.% C show graphite as an equilibrium phase, the composite matrix can be considered a typical ferrous material, with minimal influence from niobium carbide on the remaining equilibrium phases. Thus, after exceeding the necessary graphite amount to convert all niobium into NbC, we can expect the composite to have a ferrous matrix consisting of ferrite, pearlite, cementite, or graphite lamellae.

Based on Fig. 2, we varied the carbon content for the composite between 5.5 wt.% and 7.0 wt.%, corresponding to ~50 wt.% NbC and ferrous matrices ranging from fully ferritic to hypoeutectic in composition. The chosen sintering temperatures were 1150°C, just below the eutectic temperature (1169°C) to avoid permanent liquid phase formation during sintering, and 1250°C, above the eutectic temperature, leading to permanent liquid phase formation (i.e. liquid phase that is stable upon equilibrium and not caused due to local composition gradient) in samples with more than 6 wt.% C.

Fig. 3 illustrates the microstructure of composites with 5.5 to 7.0 wt.% graphite sintered at 1150 and 1250°C. All samples completed the reaction, with XRD results confirming that the composites consist of ferrite (ICSD 53451) and NbC (ICSD 94449) only, as illustrated in Fig. 4.

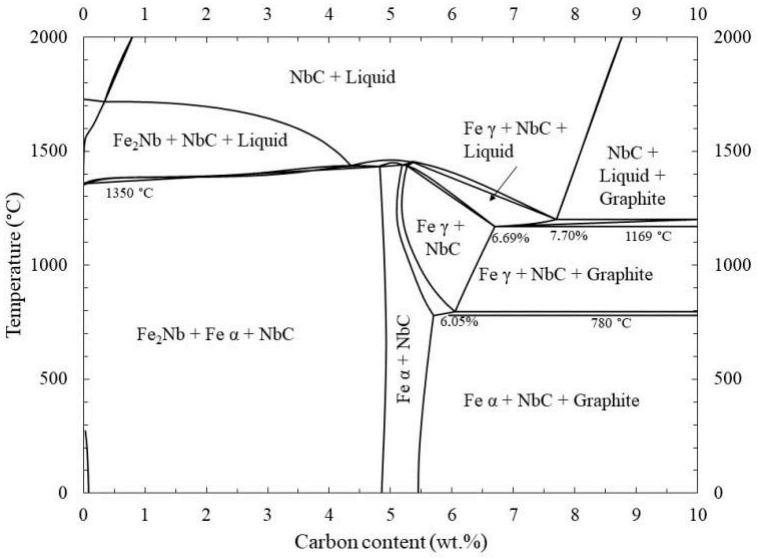

Fig. 2: Simulated pseudobinary 54.2Fe-44.5Nb-0.6Si-0.4Al-0.2Ti-C phase diagram.

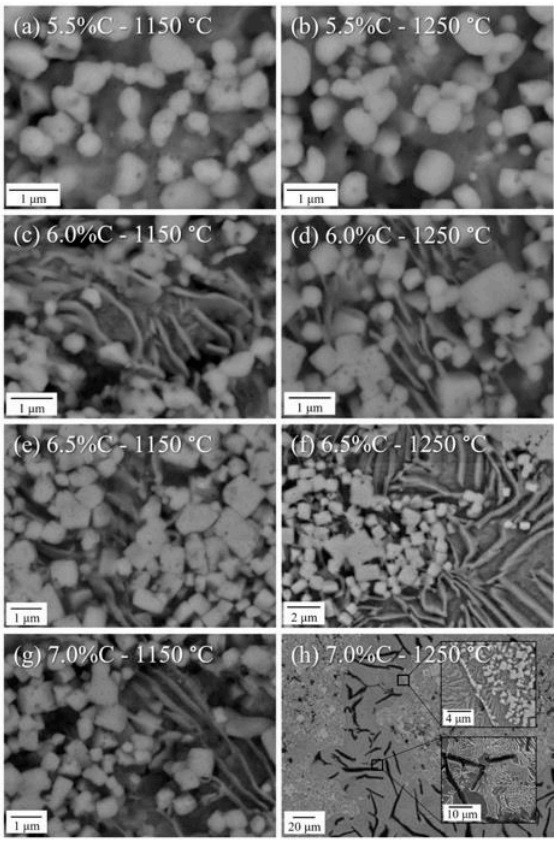

Fig. 3: Cross-sectional micrographs of composites with graphite content ranging from 5.5 to 7 wt.% and sintering temperatures from 1150 to 1250°C. Samples were etched with Nital 2%, and images captured by SEM-BSE.

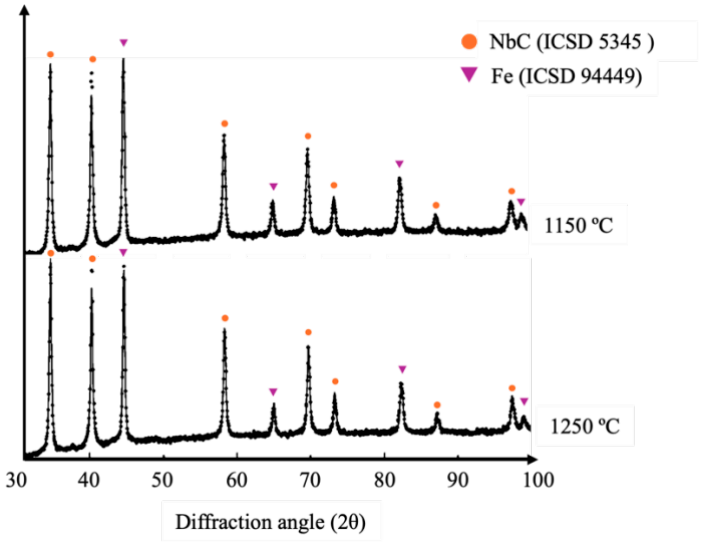

Fig. 4: X-ray diffractogram of Fe_2Nb powder reacted with 6% graphite for 1h at 1150ºC. The detected phases were NbC and α-Fe, corresponding to ICSD card numbers 5345 and 94449, respectively.

Increasing graphite content to 6.0 wt.% changes the matrix from ferritic to pearlitic, as expected for a ferrous matrix cooled from the eutectoid composition. Despite the change in the matrix phase, the distribution of carbides remains consistent, with precipitates homogeneously dispersed throughout the material. However, at 1250ºC, the carbides exhibit a more cubic morphology, likely due to the formation of a transient liquid phase caused by local compositional gradients when the reaction between graphite and Fe2Nb is incomplete. In such cases, a reduced amount of iron may become saturated with carbon, and, above the eutectic temperature, this can lead to localized melting. This observation is consistent with the densification results discussed later in Fig. 6. For the composite with 6.5 wt.% graphite, the matrix is pearlitic, consistent with thermodynamic simulations indicating a hypereutectoid matrix. Fig. 3f shows isolated pearlitic regions in the composite sintered at 1250°C, with detailed distribution shown in Fig. 5a. At 1250 ºC there is formation of permanent liquid phase was generated upon sintering .The composite with 7.0 wt.% graphite sintered at 1150°C has a similar microstructure to the 6.5 wt.% graphite composite. At 1250°C, it presents isolated regions resembling cast iron, as shown in Fig. 5b. This liquid agglomerated and formed isolated regions with negligible amounts of niobium carbide – that is, non-reinforced regions. Thus, carbides were homogeneously dispersed throughout the matrix whenever they were formed without the presence of a liquid phase, its shape was approximately spherical, with size in the order of 1µm. When liquid formation occurred, the carbides exhibited a cuboidal morphology and abnormal grain growth, with some particles exceeding 10 µm.

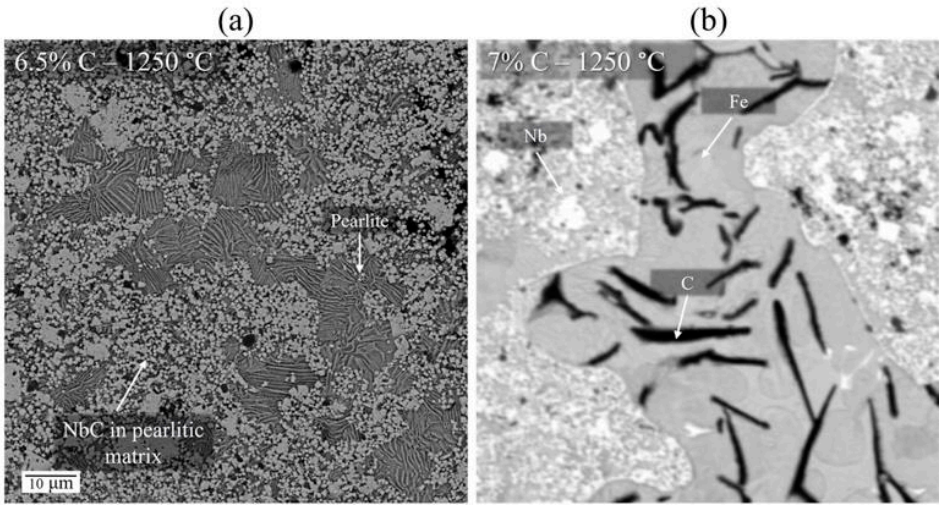

Fig. 5: (a) Microstructure of the composite with 6.5 wt.% graphite sintered at 1250°C, showing dispersed niobium carbides and pearlitic regions without carbides. (b) Cast iron islands in the composite with 7.0 wt.% graphite sintered at 1250°C.

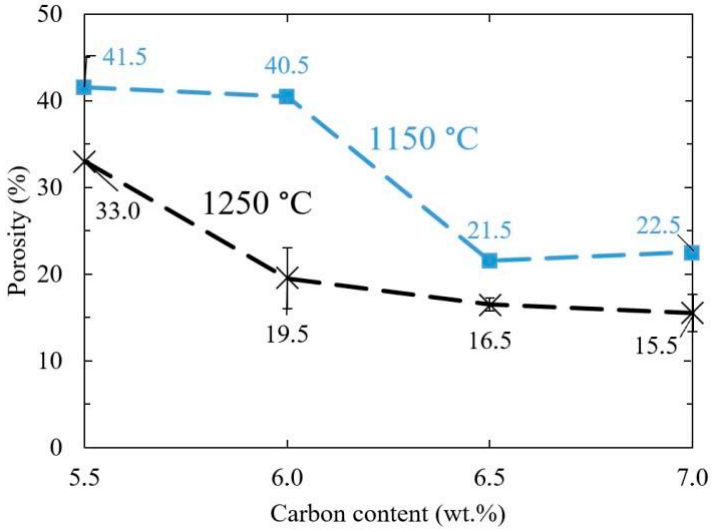

Fig. 6: Composite porosity as a function of graphite content. Increasing carbon content and sintering temperature reduces the density.

Fig. 6 shows the porosity of composites with graphite content between 5.5 and 7.0 wt.% C, sintered at 1150 and 1250°C. Before paraffin extraction and sintering, all green samples had an average porosity of 37.5 ± 0.7%. The overall high porosity fraction might be due to the limited plastic deformation capacity of the ferroniobium powder, resulting in low green density during the compaction stage. Composites with 5.5 and 6.0 wt.% C show slightly higher porosity after sintering at 1150°C than in the green state, due to paraffin extraction without significant volumetric shrinkage. Fig. 7a shows homogeneously distributed small pores (~1 µm) in the composite with 5.5 wt.% graphite sintered at 1250°C, likely corresponding to voids within each granule. Increasing graphite content to 6.5 wt.% reduces porosity abruptly to 21.5 ± 0.7%, with a similar value for 7 wt.% graphite. At 1250°C, the composite with 5.5 wt.% graphite densifies slightly, but porosity remains at 33.0 ± 0.7%. Increasing carbon to 6.0 wt.% at 1250°C reduces porosity to 19.5 ± 0.7%, possibly due to transient liquid phase. Literature reports morphology shifts from spherical or angular to cuboidal niobium carbide due to liquid phase presence [10,11]. Higher carbon content and sintering temperature tend to decrease composite porosity, especially smaller pores, as shown in Fig. 7b and Fig. 7d. The composite with 7.0 wt.% graphite sintered at 1250°C achieved the lowest porosity. The formation of isolated pearlite and cast iron regions in composites with 6.5 and 7.0 wt.% graphite at 1250°C may relate to excessive liquid phase formation during sintering, as niobium carbide's low wettability in iron causes liquid phase segregation from carbides. As little niobium is dissolved in the matrix, pearlite and cast iron form upon cooling. Cubic morphology and abnormal grain growth occur on faceted grains, potentially improving scratch and abrasion resistance, though this analysis is outside this work's scope. Larger pores, as depicted in Fig. 7c were found in all samples and may result from unfilled spaces between granules during compaction. If confirmed, adjustments in the compaction stage could significantly reduce the >15% porosity still present in composites without 1µm pores.

The hardness and microhardness values of the composites are displayed in Fig. 8. Due to the presence of porosity, there is a significant difference between the macrohardness and microhardness measurements. The composite with 6.5 wt.% carbon, sintered at 1250 °C, exhibits the highest microhardness at 952 ± 82 HV0.05, yet its macrohardness is only 466 ± 17 HV10. Macrohardness tests create indentations that cover the entire microstructure, including pores, whereas microhardness tests with a 50 gf load focus on smaller areas of the microstructure, including the carbides, matrix, and smaller pores. For composites with higher density, where a liquid phase likely formed during sintering, there are fewer pores, making the microhardness measurements more representative of the behavior of a pore-free material.

The increase in hardness with higher sintering temperatures may be attributed to a decrease in porosity. The decrease in microhardness in composites with 7.0 wt.% carbon might be due to the formation of cast iron and the coalescence of carbides.

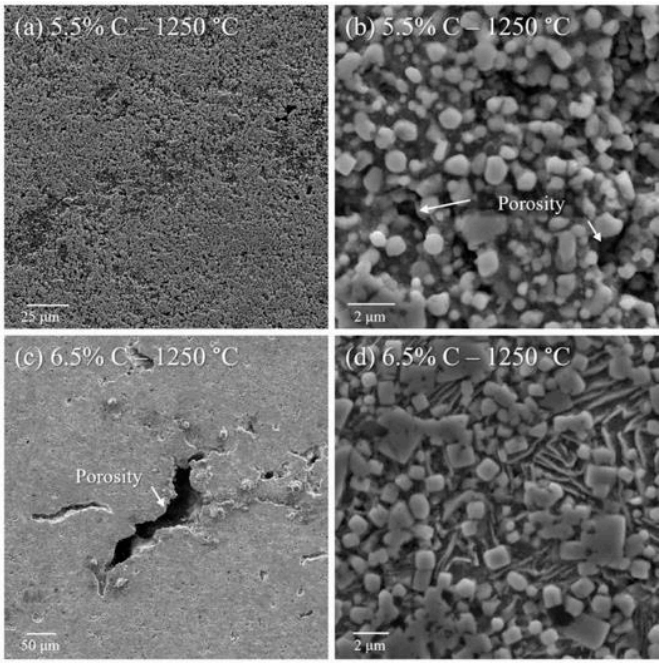

Fig. 7: Composite porosity. Without liquid phase formation, small pores from particle voids are present (a). Liquid phase formation reduces this porosity type (b) but does not mitigate pores from granule voids (c).

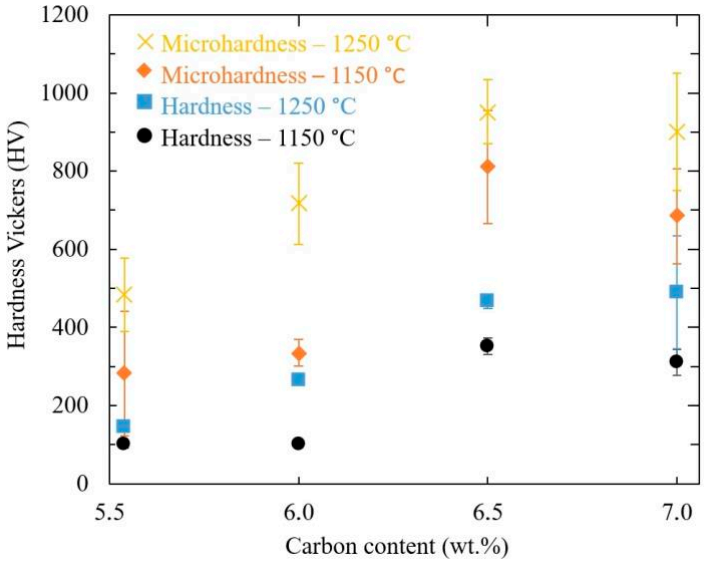

Fig. 8: Hardness measured with a load of 10 kgf, and microhardness measured with a load of 50 gf. Microhardness was measured in areas containing niobium carbide dispersed in the ferrous matrix, avoiding pearlite and cast iron islands in composites with more than 6.0 wt.% carbon sintered at 1250 °C.

Conclusion

- The interaction between Fe_2Nb powders and graphite during the sintering process results in NbC-reinforced ferrous matrix composites. Adjusting the carbon content by adding graphite (5.5-7.0 wt.%) alters the ferrous matrix composition, which can lead to the formation of a

pearlitic matrix or graphite lamellae.

- The microstructure is significantly influenced by sintering temperatures of 1150°C and 1250°C due to the formation of liquid phase. The morphology of carbides is shaped by sintering temperature, with excessive amounts of liquid causing abnormal growth of cubic carbides.

- Increasing the graphite content and sintering temperature decreases porosity and enhances hardness to some extent. However, microstructural coarsening and liquid phase formation lead to the creation of reinforcement-free zones of pearlite/cast iron, which negatively affect hardness.

- There is potential for further improvement in densification, particularly in addressing large secondary pores and compaction defects.

Acknowledgements

The authors would like to acknowledge FINEP (Financiadora de Estudos e Projetos) e CNPq (Conselho Nacional de Desenvolvimento Científico e Tecnológico) for the financial support.

References

1) Zapata A WC, Da Costa CE. Wear and thermal behaviour of M2 high-speed steel reinforced with NbC composite. Vol. 33, JOURNAL OF MATE RIALS SCIENCE. 1998.
2) Dematte E, Franco E, Milan J, Costa CE da. Influence of Milling and Use of Ni and Al Containing Metal Binder in NbC-Based Cermets. Materials Research. 2023;26.
3) Esteban PG, Gordo E. Development of Fe–NbC cermet from powder obtained by self-propagating high temperature synthesis. Powder Metallurgy. 2006 Jun 19;49(2):153–9.
4) Bolton JD, Gant AJ. Microstructural development and sintering kinetics in ceramic reinforced high speed steel metal matrix composites. Powder Metallurgy. 1997;40(2):143–51.
5) Li S, Kondoh K, Imai H, Chen B, Jia L, Umeda J, et al. Strengthening behavior of in situ-synthesized (TiC-TiB)/Ti composites by powder metallurgy and hot extrusion. Mater Des. 2016 Apr 5;95:127–32.
6) Ziemnicka-Sylwester M. The Cu matrix cermets remarkably strengthened by TiB2 ‘in situ’ synthesized via self-propagating high temperature synthesis. Mater Des. 2014;53:758–65.
7) Jia L, Chen B, Li SF, Imai H, Kondoh K. Pinning effect of in-situ TiCp and TiBw on the grain size and room temperature strength of (TiC + TiB)/Ti composites. KONA Powder and Particle Journal. 2015;(32):264–9.
8) Huth S, Theisen W. Diffusion alloying – a new manufacturing method for PM tool steels. Powder Metallurgy. 2009 Jun 19;52(2):90–3.
9) Huth S, Krasokha N, Theisen W. Development of wear and corrosion resistant cold-work tool steels produced by diffusion alloying. Wear. 2009 Jun;267(1–4):449–57.
10) Franco E, da Costa CE, Tsipas SA, Gordo E. Cermets based on FeAl–NbC from composite powders: Design of composition and processing. Int J Refract Metals Hard Mater. 2015 Jan;48:324–32.
11) Woydt M, Huang S, Vleugels J, Mohrbacher H, Cannizza E. Potentials of niobium carbide (NbC) as cutting tools and for wear protection. Int J Refract Metals Hard Mater. 2018 Apr 1;72:380–7.

Received June 30, 2024; Revised October 7, 2024; Accepted October 9, 2024